

Complex photonic graphene: Optical tachyons, strain, and \mathcal{PT} -symmetry

Alexander Szameit, Mikael C. Rechtsman, Omri Bahat-Treidel, and Mordechai Segev

Physics Department and Solid State Institute, Technion, 32000 Haifa, Israel

Abstract

We apply gain/loss to honeycomb photonic lattices and demonstrate that optical tachyons, a photonic version of particles that travel faster than the speed of light, can be generated by \mathcal{PT} -symmetry breaking in this structure. We further show that the \mathcal{PT} -symmetry can be restored via strain.

Honeycomb photonic lattices [1] - the optical version of the well known graphene [2] (a monolayer of carbon atoms arranged in a honeycomb geometry) - shares many common features with that unique material. Interestingly, such “photonic graphene” actually displays several additional phenomena that do not exist in the original electronic system, for example, conical diffraction by virtue of symmetry [2]. When transferring the physics of particles onto an analogous optical setting, which is justified by the fundamental wave-particle duality, the observer benefits from spatial (rather than temporal) evolution and from almost arbitrary scalability of the refractive index contrast, compared to the atomic potential. Furthermore, the wave function and its evolution can be directly imaged and monitored as they evolve. In this vein, it was recently suggested to study Klein tunnelling in honeycomb photonic lattices [3]. Importantly, optical systems offer the possibility of employing nonlinearity, which has significant impact on the wave packet evolution [4].

In a different area, complex non-conservative systems, which, under special conditions, may exhibit non-Hermitian, but \mathcal{PT} -symmetric, Hamiltonians, have garnered growing scientific interest in recent years. \mathcal{PT} -symmetric systems are characterized by a complex potential, which has neither parity symmetry (\mathcal{P}) nor time-reversal symmetry (\mathcal{T}), yet the Hamiltonian commutes with \mathcal{PT} , and the system’s eigenstates simultaneously diagonalize \mathcal{PT} and the Hamiltonian [5]. Under these conditions, the eigenvalues of the Hamiltonian are real, in spite of the fact that the potential is complex [5]. Such systems were introduced into the domain of optics, which provides exceptional conditions to observe \mathcal{PT} -symmetric systems [6]. It turned out that \mathcal{PT} -symmetry plays an important role in the light evolution in optical systems [7]. Their simplest realization occurs for two identical coupled waveguides, one with gain and the other with loss,

such that the real part of the refractive index is symmetric with respect to the interchange of waveguides whereas the imaginary counterpart is anti-symmetric. This realization was recently demonstrated in experiments [8], although some of the underlying effects were observed even without gain, when both waveguides contain unequal loss [9].

Here, we show that adding gain/loss to a regular photonic honeycomb lattice – small as it may be – can never result in \mathcal{PT} -symmetry. However, this unique system can support the formation of optical tachyons – a photonic version of hypothetical particles with imaginary mass and a group velocity exceeding the vacuum speed of light. Nevertheless, applying a strain to the honeycomb lattice restores \mathcal{PT} -symmetry, in particular in the most interesting region of the band structure: the vicinity of the Dirac points.

The structure of complex photonic graphene – a honeycomb arrangement of waveguides with alternating gain/loss – is sketched in Fig. 1a. In our lattice, we assume a linear strain t in the horizontal direction, with $t=1$ as the unperturbed structure [4]. Additionally, one may introduce a detuning Δ in the effective index between adjacent guides. A honeycomb lattice is composed of two displaced hexagonal sublattices a and b . Therefore, in a tight-binding model, the dynamics of the entire system can be described by the equations [4]

$$\begin{aligned} i\partial_z a_{m,n} &= -\Delta a_{m,n} - i\gamma a_{m,n} + c(tb_{m-1,n} + b_{m,n+1} + b_{m,n-1}) \\ i\partial_z b_{m,n} &= +\Delta b_{m,n} + i\gamma b_{m,n} + c(ta_{m+1,n} + a_{m,n+1} + a_{m,n-1}) \end{aligned} \quad (1)$$

where c is the coupling constant between adjacent guides. The quantity γ describes the gain and loss of the waveguides in the a and b sublattices. The spectrum of the eigenvalues $\beta(\mu, \nu)$ can be obtained by substituting the plane wave solutions $a_{m,n} = A \exp\{i(\beta z + \sqrt{3}\mu m + \nu n)\}$, and

$b_{m,n} = B \exp\{i(\beta z + \sqrt{3}\mu m + \nu n)\}$ into Eq. (1), where μ and ν represent the transverse wave vectors, A and B are amplitudes, and the factor $\sqrt{3}$ results from the lattice structure. This results in the eigenvalue problem

$$\begin{pmatrix} \Delta + i\gamma & cte^{-i\sqrt{3}\mu} + 2c \cos \nu \\ cte^{i\sqrt{3}\mu} + 2c \cos \nu & -\Delta - i\gamma \end{pmatrix} \begin{pmatrix} A \\ B \end{pmatrix} = \beta \begin{pmatrix} A \\ B \end{pmatrix}, \quad (2)$$

yielding the dispersion relation for the propagation constant β , which describes the rate of phase evolution in the propagation direction:

$$\beta = \pm \sqrt{\Delta^2 - \gamma^2 + 2i\gamma\Delta + c^2t^2 + 4c^2 \cos^2 \nu + 4tc^2 \cos \nu \cos \sqrt{3}\mu}. \quad (3)$$

Ideal (unperturbed) photonic graphene is obtained for $\Delta=\gamma=0$ and $t=1$, and its dispersion relation is shown in Fig. 1b. One of the striking features of the band structure of this system is the existence of the so-called Dirac region in the vicinity of the intersection points (the vertices) between the first and the second bands. In this regime the Hamiltonian of the system – defined in Eq. (2) – can be expanded around the vertices into a Taylor series [10], resulting in a mathematical structure similar to the one in the relativistic Dirac equation, which describes relativistic quantum particles:

$$H = f(t)\tilde{\nu}\sigma_1 + ct\sqrt{3}\tilde{\mu}\sigma_2 + (\Delta + i\gamma)\sigma_3. \quad (4)$$

Here, $\sigma_{1,2,3}$ are the Pauli matrices:

$$\sigma_1 = \begin{pmatrix} 0 & 1 \\ 1 & 0 \end{pmatrix}; \quad \sigma_2 = \begin{pmatrix} 0 & -i \\ i & 0 \end{pmatrix}; \quad \sigma_3 = \begin{pmatrix} 1 & 0 \\ 0 & -1 \end{pmatrix} \quad (5)$$

and $f(t) = 2c\sqrt{1-t^2/4}$. The quantities $\tilde{\mu} = \mu - \mu_0$ and $\tilde{\nu} = \nu - \nu_0$ are transverse wave vectors measured from the position of the given Dirac point $[\mu_0, \nu_0]$. Note that the regime of validity is $t < 2$ [3]. In Eq. (4), the detuning Δ plays the role of a mass of a relativistic fermion in Dirac's

theory, whereas the gain/loss factor γ represents an *imaginary* mass. The Dirac region for $\Delta=\gamma=0$, resembling the dispersion relation of a massless particle, is shown in Fig. 1(c). In contrast, when both sublattices a and b are detuned by $\Delta>0$, a gap opens between the two bands, as shown in Fig. 1(d), where $\Delta=0.2$. The magnified Dirac region (see Fig. 1(e)) reveals a parabolic shape of the dispersion relation, indicating the resemblance of the dispersion of a massive relativistic particle.

The situation changes drastically when gain and loss are introduced to the system. Whereas for $\gamma=0$ the Hamiltonian is Hermitian, resulting in a purely real eigenvalue spectrum, a gain/loss structure with $\gamma>0$ results in a non-Hermitian Hamiltonian that in general exhibits a non-real eigenvalue spectrum. Exactly this happens in photonic graphene, where according to Eq. (3) one finds that (if $\Delta=0$ and $t=1$) for every γ there exist imaginary β in the Dirac region. In more technical terms, complex eigenvalues of the Hamiltonian appear when its eigenvectors do not simultaneously diagonalize \mathcal{PT} . Such a system is said to have broken \mathcal{PT} -symmetry, although the \mathcal{PT} operator still commutes with the Hamiltonian. This seeming paradox stems from the fact that the \mathcal{T} operator is an anti-linear operator. A graph of the real part of the dispersion relation with $\gamma=0.5$ is shown in Fig. 2a, and a magnification of the Dirac region is shown in Fig. 2b. In contrast to "conventional" graphene, the dispersion is now hyperbolic. Figures 2c,d show the imaginary part of the dispersion relation and the magnification of the Dirac region, indicating purely imaginary eigenvalues around the original vertices. Note that there is no detuning between the sublattices a and b , i.e. $\Delta=0$. If the structure exhibits both detuning and gain/loss (i.e. $\Delta>0$, $\gamma>0$) then, according to Eq. (3) all eigenvalues are complex due to the term $2i\gamma\Delta$.

Interestingly, Eq. (4) suggests that our system resembles the dynamics of relativistic particles with imaginary rest mass – generally known as tachyons [11]. Tachyons are hypothetical particles that exhibit various peculiar features; the most striking is that they travel faster than the vacuum speed of light. Furthermore, these strange particles get faster the lower their energy is, and approach an infinite velocity when their energy is zero. Note that – if tachyons were conventional, localizable, particles – they could be used to send signals faster than light, which would, however, lead to violations of causality. A full discussion of applications for tachyons (albeit somewhat speculative) can be found in [12]. Currently, according to the contemporary and widely accepted understanding of the concept of a particle, tachyon particles are assumed to be non-existent [13]. Nevertheless, despite the theoretical arguments against the existence of tachyons, no clear experimental evidence for or against their existence has been found [14].

Photonic graphene with a gain/loss structure provides a classical optical analogue of tachyons, which can be experimentally probed in a table-top experiment. First evidence is given by the fact that the gain/loss factor γ can be interpreted as an imaginary mass due to its appearance on the main diagonal of the Dirac Hamiltonian in Eq. (4). Additionally, an intuitive understanding of the analogous behavior of an optical wave packet in photonic graphene and tachyons in vacuum can be gathered by analyzing the hyperbolic dispersion relation. In Fig. 3a, we show a cross section of the real part of the dispersion relation through the Dirac region. The transverse velocity of a wave packet, which is defined as the gradient of the dispersion relation and is equivalent to the group velocity [15], increases strongly above the values for "conventional" photonic graphene in the Dirac region, and diverges when the propagation constant β approaches zero (see Fig. 3b). Note that the propagation constant β of an optical wave

packet is the optical analogue of the quantum mechanical energy of an evolving particle. Therefore, a wave packet associated with the regions where $\beta \rightarrow 0$ will travel with a group velocity far beyond the speed of corresponding wave packets in "conventional" photonic graphene.

We test our analytical results in numerical simulations by evaluating the displacement of a very broad wave packet after some propagation, as a function of the transverse wave vector μ . The results are summarized in Fig. 3c, comparing the final position of a propagated wave packets in the cases $\gamma=0$ and $\gamma=0.5$. Indeed, in the gain/loss system the transverse displacement of the wave packet is larger. In Fig. 3d, the transverse speed of a propagating wave packet is plotted as a function of the initial transverse momentum, showing highly convincing evidence for the predicted tachyonic behavior: in the Dirac region the transverse speed of the wave packet in the gain/loss system clearly exceeds the speed of a wave packet in conventional photonic graphene, defined by the constant slope of the linear dispersion. The wave packet travels faster than the optical analogue of the speed of light in the Dirac equation. Note that close to the point where β is close to zero and becomes imaginary, the numerically obtained group velocity of the wave packet deviates from the analytical prediction. We attribute this fact to the finite width of our wave packet: the region in reciprocal space, where the velocities diverge, is very narrow. Consequently, due to its finite spectral width in the transverse direction, the wave packet used in the simulations inevitably displays an average over this region in momentum space. Nevertheless, our system clearly exhibits superluminal characteristics – the gain/loss structure of complex photonic graphene allows the formation of optical tachyons – superluminal beams

propagating at angles steeper than dictated by the underlying honeycomb lattice - which can be studied in table-top experiments.

Finally, we point out that the strain t , as defined in Eq. (1), is capable of restoring the \mathcal{PT} -symmetry in this complex photonic graphene. In conventional photonic graphene ($\Delta=\gamma=0$), increasing the strain forces the Dirac points to move towards each other until they merge at $t=2$ [6]. Using Eq. (3), one can easily show that, for vanishing detuning ($\Delta=0$), for any given gain/loss factor γ - all eigenvalues of β become real above a threshold strain $t \geq 2 + (\gamma/c)$. Therefore, in such a setting, the structure is fully \mathcal{PT} -symmetric, and critical points appear exactly for $t=2+\gamma$. The Hamiltonian of this system reads [3]

$$H = \left[2(t-2) - 3ct\tilde{\mu}^2 + c\tilde{\nu}^2 \right] \sigma_1 + ct\sqrt{3}\tilde{\mu}\sigma_2 + (\Delta + i\gamma)\sigma_3. \quad (6)$$

Note that the quadratic term $\sim \tilde{\mu}^2$ may not be neglected since the dispersion obtained from (6) must coincide with the expansion of (3). In Fig. 4a, we show the dispersion relation for photonic graphene, with no detuning ($\Delta=0$), but with gain/loss structure ($\gamma=0.5$), and additional strain $t = 2 + (0.5/c)$ compensating for the imaginary part of Eq. (3). In the magnified view of the Dirac region (see Fig. 4b), one finds that for this particular strain yields a vertex at the center of the Dirac region and a linear, but anisotropic, dispersion in μ and ν . However, for a slightly larger strain $t = 2 + (0.55/c)$ - all eigenvalues β remain real, but a gap opens between both bands, as depicted in Fig. 4c. The magnification of the Dirac region, shown in Fig. 4d, reveals that sufficiently away from the former vertex, the dispersion relation is still linear and anisotropic in μ and ν . Hence, a beam with eigenvalues close to the vertex will propagate with constant amplitude in the \mathcal{PT} -symmetric system since its total energy is conserved, whereas in the

unstrained system the beam will experience an amplitude growth beyond all limits due to the imaginary eigenvalues, as shown in Fig. 5.

In conclusion, we described the properties of complex photonic graphene and revealed its potential to support optical tachyons. Whereas \mathcal{PT} -symmetry is always broken in undeformed complex graphene, all eigenvalues may be rendered real by introducing a sufficiently strong linear strain, thereby restoring the \mathcal{PT} -symmetry. Besides the potential of optical graphene as a classical simulator for relativistic physics [16], in contrast to quantum simulators [16, 17], we envision various applications, in particular for dielectric nonreciprocal optical elements, with no net loss.

This work was sponsored by an Advanced Grant from the European Research Council (ERC), by the Israel Science Foundation, by the German-Israeli Foundation (GIF). AS acknowledges support by the German Academy of Science Leopoldina (grant LPDS 2009-13). MCR is grateful to the Azrieli foundation for the award of an Azrieli fellowship.

References

- [1] O. Peleg, G. Bartal, B. Freedman, O. Manela, M. Segev and D. N. Christodoulides, Phys. Rev. Lett **98**, 103901 (2007).
- [2] K. S. Novoselov, A. K. Geim, S. V. Morozov, D. Jiang, Y. Zhang, S. V. Dubonos, I. V. Grigorieva, A. A. Firsov, Science **306**, 666-669 (2004).
- [3] O. Bahat-Treidel, O. Peleg, M. Grobman, N. Shapira, T. Pereg-Barnera, and M. Segev, Phys. Rev. Lett. **104**, 063901 (2010).
- [4] M. J. Ablowitz, S. D. Nixon, and Y. Zhu, Phys. Rev. A **79**, 053830 (2009); O. Bahat-Treidel, O. Peleg, M. Segev, and H. Buljan, Phys. Rev. A **82**, 013830 (2010).
- [5] C. M. Bender and S. Böttcher, Phys. Rev. Lett. **80**, 5243-5246 (1998).
- [6] R. El-Ganainy, K. G. Makris, D. N. Christodoulides, and Ziad H. Musslimani, Opt. Lett. **32**, 2632-2634 (2007); K.G. Makris, R. El-Ganainy, D. N. Christodoulides, and Ziad H. Musslimani, Phys. Rev. Lett. **100**, 103904 (2008); S. Klaiman, U. Günther, and N. Moiseyev, Phys. Rev. Lett. **101**, 080402 (2008).
- [7] S. Longhi, Phys. Rev. Lett. **103**, 123601 (2009); S. Longhi, Phys. Rev. B **80**, 235102 (2009).
- [8] C. Rüter, K. G. Makris, R. El-Ganainy, D. N. Christodoulides, M. Segev, and D. Kip, Nature Phys. **6**, 192-195 (2010).
- [9] A. Guo, G. J. Salamo, D. Duchesne, R. Morandotti, M. Volatier-Ravat, V. Aimez, G. A. Siviloglou, and D. N. Christodoulides, Phys. Rev. Lett. **103**, 093902 (2009).
- [10] S.-L. Zhu, B. Wang, and L. M. Duan, Phys. Rev. Lett. **98**, 260402 (2007).
- [11] O.-M. P. Bilaniuk and E. C. G. Sudarshan, Phys. Today **22**, 43–51 (1969); O.-M. P. Bilaniuk, V. K. Deshpande, and E. C. G. Sudarshan, Am. J. Phys. **30**, 718-??? (1962); G. Feinberg, Phys. Rev. **159**, 1089–1105 (1967).

- [12] R. Sternbach and M. Okuda, *Star Trek – The Next Generation: The Technical Manual*, Boxtree Ltd. publishing (1991).
- [13] M. E. Peskin and D. V. Schroeder, *An Introduction to Quantum Field Theory*, Perseus books publishing (1995).
- [14] G. Feinberg, “Tachyon” article in *Encyclopedia Americana*, Grolier Incorporated, vol. **26**, p. 210 (1997).
- [15] H. S. Eisenberg, Y. Silberberg, R. Morandotti, and J. S. Aitchison, Phys. Rev. Lett. **85**, 1863-1866 (2000).
- [16] F. Dreisow, M. Heinrich, R. Keil, A. Tünnermann, S. Nolte, S. Longhi, and A. Szameit, Phys. Rev. Lett. **105**, 143902 (2010).
- [17] R. Gerritsma, G. Kirchmair, F. Zähringer, E. Solano, R. Blatt, and C. F. Roos, Nature **463**, 68 (2010); R. Gerritsma, B. P. Lanyon, G. Kirchmair, F. Zähringer, C. Hempel, J. Casanova, J. J. García-Ripoll, E. Solano, R. Blatt, and C. F. Roos, Phys. Rev. Lett. **106**, 060503 (2011)

Figure Captions:

Fig. 1.

(a) Sketch of complex photonic graphene. The red and blue waveguides exhibit gain and loss, respectively. Additionally, a strain can be applied along the horizontal direction. (b) The dispersion relation of conventional photonic graphene, where $\Delta=\gamma=0$. (c) The magnified conical Dirac region, resembling the dispersion relation for a massless relativistic particle. (d) The dispersion relation of photonic graphene, where $\gamma=0$, but $\Delta=0.2$. (e) The magnified Dirac region, resembling the dispersion relation for a massive relativistic particle.

Fig. 2:

(a) The real part of the dispersion relation of photonic graphene for $\gamma=0.5$ and $\Delta=0$. (b) A magnified view on the hyperbolic shape of the real part of β , which is described by a Dirac equation for particles with imaginary mass. (c) A plot of the imaginary part of the dispersion relation, showing the eigenvalues β become imaginary in the vicinity of the Dirac points. (d) A magnified view of the imaginary eigenvalues in the Dirac region.

Fig. 3:

(a) A cross section through the real part of the dispersion relation in Fig. 1(b) along μ for $\nu=0$. (b) The slope of (a), that diverges in the vicinity of the Dirac region, indicating transverse speeds exceeding that in conventional graphene. (c) Comparison of the initial position of the wave packet with momentum $[\mu=0; \nu=0.5\pi]$ (black solid line) and the final position when $\gamma=0$ (red dotted line) and $\gamma=0.5$ (blue dashed line). (d) Numerical simulation of the transverse

displacement of a wave packet as a function of the initial transverse momentum (red solid line) compared to the analytic solution (blue dashed line). Speeds exceeding the maximal value in conventional photonic graphene (black dotted line) correspond to tachyonic behavior.

Fig. 4:

(a) Dispersion relation for $\gamma=0.5$ and $t = 2 + (0.5/c)$. All eigenvalues β are real, despite the complex potential, indicating that the structure exhibits \mathcal{PT} -symmetry. (b) The enlarged Dirac region, where a vertex exists and the dispersion is linear in both μ and ν , but anisotropic. (c) Dispersion relation, when the strain is increased to $t = 2 + (0.55/c)$. All eigenvalues β remain real, but a gap opens between both bands. (d) The enlarged Dirac region shows that, sufficiently away from the former vertex, the dispersion remains linear and anisotropic in both μ and ν .

Fig. 5:

Comparison of the amplitude of a propagating wave packet for $\gamma=0.5$ with momentum $[\mu=0; \nu=0.6\pi]$ and no strain $t=0$ (black solid line), and in the same region for $t=t_c$ when \mathcal{PT} -symmetry is restored and all eigenvalues are real (red dashed line).

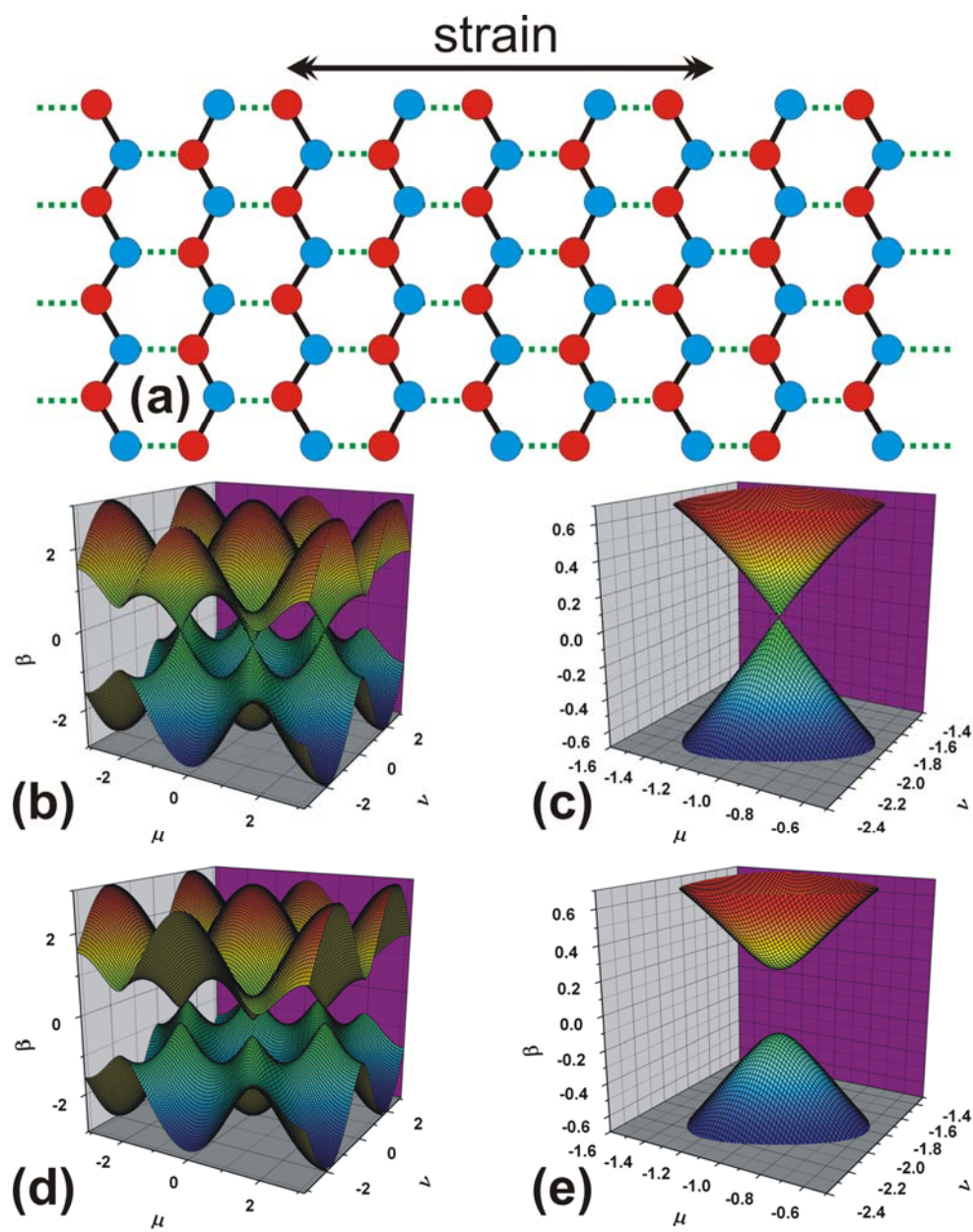


Figure 1

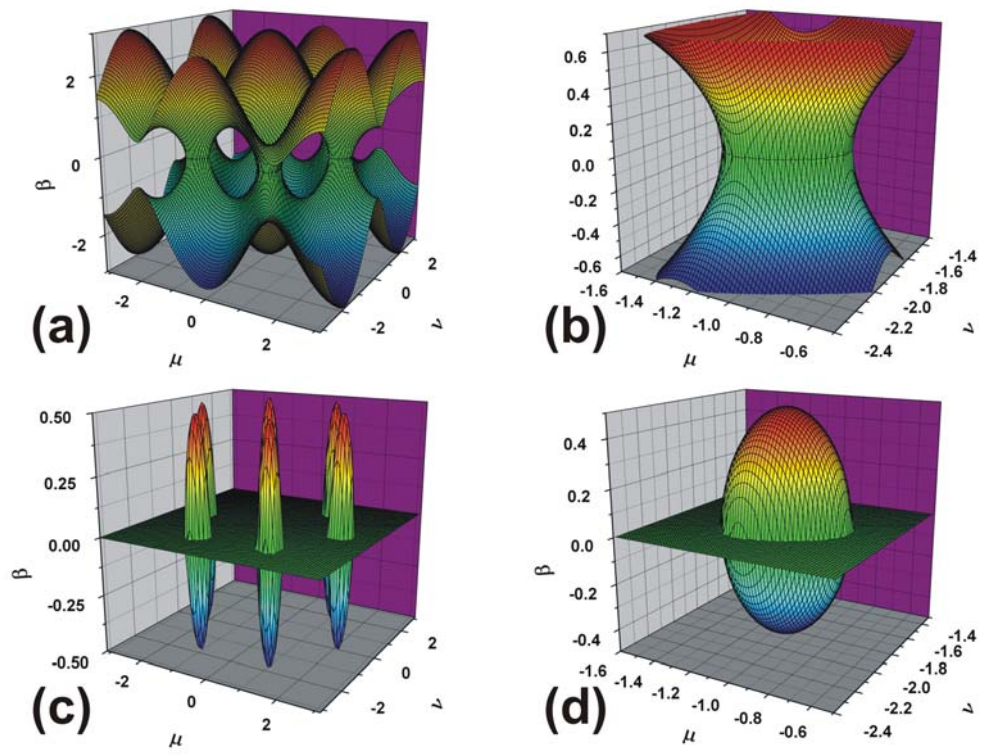


Figure 2

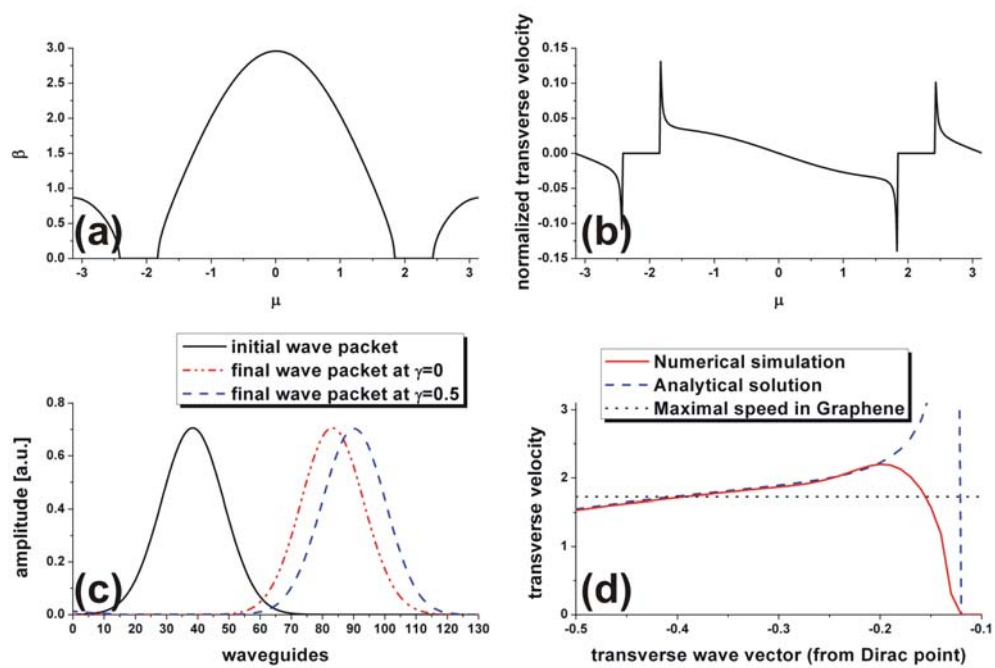


Figure 3

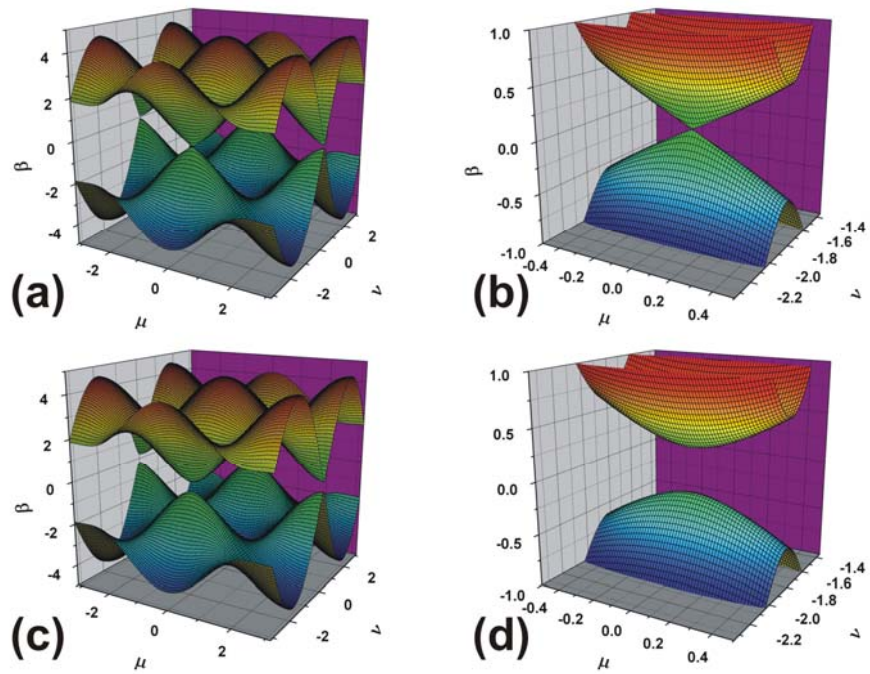


Figure 4

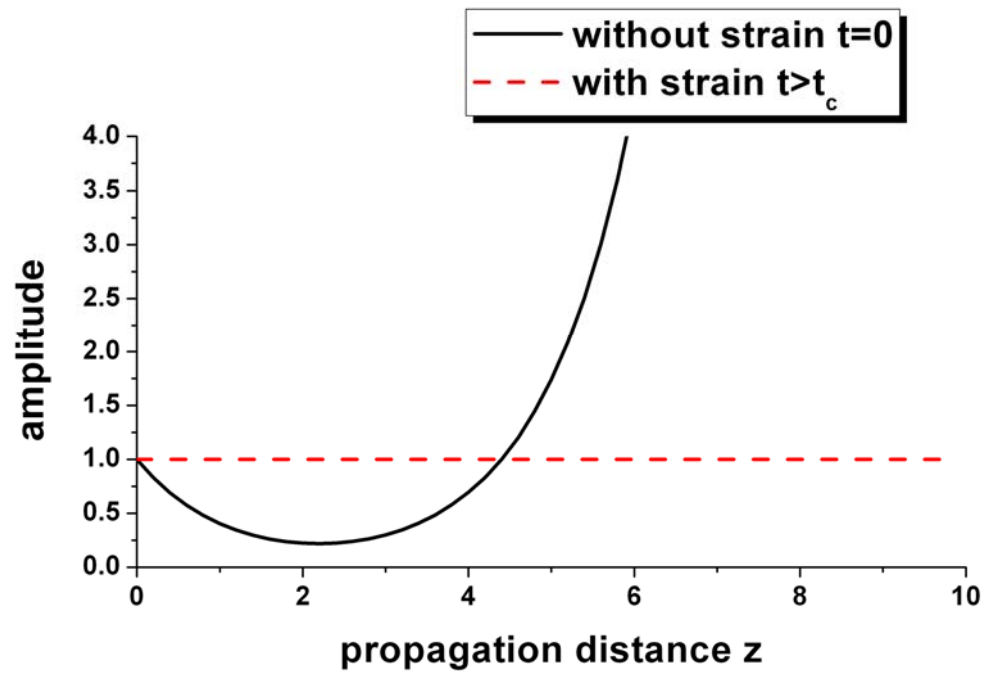


Figure 5